NASA TECHNICAL MEMORANDUM

NASA TM X-2756

NASA TM X-2756

ELECTRON EMISSION PRODUCED BY PHOTOINTERACTIONS IN A SLAB TARGET

by Byron E. Thinger and James A. Dayton, Jr.

Lewis Research Center
Cleveland, Ohio 44135

NATIONAL AERONAUTICS AND SPACE ADMINISTRATION • WASHINGTON, D. C. • MARCH 1973

1. Report No.	2. Government Accession No.	3. Recipient's Catalog No.
NASA TM X-2756		

4. Title and Subtitle	5. Report Date
ELECTRON EMISSION PRODUCED BY PHOTOINTERACTIONS IN A SLAB TARGET	March 1973
	6. Performing Organization Code

7. Author(s)	8. Performing Organization Report No.
Byron E. Thinger, California State University, San Francisco, California; and James A. Dayton, Jr., Lewis Research Center	E-7265
	10. Work Unit No. 503-25
9. Performing Organization Name and Address Lewis Research Center National Aeronautics and Space Administration Cleveland, Ohio 44135	11. Contract or Grant No.
	13. Type of Report and Period Covered Technical Memorandum
12. Sponsoring Agency Name and Address National Aeronautics and Space Administration Washington, D.C. 20546	14. Sponsoring Agency Code

15. Supplementary Notes

16. Abstract

The current density and energy spectrum of escaping electrons generated in a uniform plane slab target which is being irradiated by the gamma flux field of a nuclear reactor are calculated by using experimental gamma energy transfer coefficients, electron range and energy relations, and escape probability computations. The probability of escape and the average path length of escaping electrons are derived for an isotropic distribution of monoenergetic photons. The method of estimating the flux and energy distribution of electrons emerging from the surface is outlined, and a sample calculation is made for a 0.33-cm-thick tungsten target located next to the core of a nuclear reactor. The results are to be used as a guide in electron beam synthesis of reactor experiments.

17. Key Words (Suggested by Author(s))	18. Distribution Statement
Secondary emission; Photointeraction; Gamma ray absorption; Probability of escape; Nuclear reactor; Thermionic conversion; Electron beam	Unclassified - unlimited

19. Security Classif. (of this report)	20. Security Classif. (of this page)	21. No. of Pages	22. Price*
Unclassified	Unclassified	18	$3.00

* For sale by the National Technical Information Service, Springfield, Virginia 22151

ELECTRON EMISSION PRODUCED BY PHOTOINTERACTIONS IN A SLAB TARGET

by Byron E. Thinger* and James A. Dayton, Jr.

Lewis Research Center

SUMMARY

A method of estimating the production and penetration of energetic electrons in a target as a consequence of photon interactions is described. The calculations incorporate the experimentally determined photoelectric, Compton, and pair production interaction cross sections and utilize empirical electron energy range relations. The prediction of energetic electron emission is based on two quantities which are derived in this report, the probability of electron escape and the average path length of escaping electrons.

In this analysis the fission gamma energy spectrum is divided into multiple energy groups, each of which is defined in terms of a monoenergetic gamma flux. With the mean energy of each gamma group as a reference, the number and average energy of primary electrons produced within the target are determined. The transport and loss of energy of those electrons which are able to travel through the target to the surface are computed to give the power per unit area of the emerging electrons and the corresponding escape current density. These latter two quantities are of interest in an application to thermionic conversion within a nuclear reactor system.

The results are presented for a numerical computation of the current density and energy flux of the electrons emitted from a 0.33-centimeter-thick tungsten target irradiated in the core of the NASA Lewis Research Center Plum Brook nuclear test reactor.

INTRODUCTION

The ionizing effects of gamma radiation have been studied as a means of reducing the plasma impedance of in-core nuclear thermionic convertors by Butler (ref. 1) and

*Assistant Professor of Engineering, California State University, San Francisco, California; Summer Faculty Fellow at the Lewis Research Center in 1969.

Forman (ref. 2). Gas-filled electronic tubes appear to conduct more current when they are operated in or near a nuclear reactor. Presumably the conductivity of the filling gas is increased because of ionization of the neutral gas atoms by energetic photons and by electrons generated by the interaction of gamma rays with the tube surfaces. Forman's initial reactor experiments indicated some promise for thermionic converter performance improvement. However, Butler's analysis predicts that the ionization contributed by the gamma radiation field is small, and no enhancement of operation could be expected.

The primary objective of this work is to calculate the current density and energy spectra of electrons which are emitted from the surface of a metal target placed in the gamma radiation field in the core of a nuclear reactor. Since experiments within nuclear reactors are quite costly and require extensive hazards analysis and lead time, other methods of studying the effects of gamma radiation on the performance of thermionic converters are of interest. For instance, one method might be to simulate the yield of primary electrons from a target by using the beam from a linear accelerator, for example, the 3-Mev linear accelerator at the Lewis Research Center. The procedure would involve first calculating the energy (velocity) distribution of primary electrons that are emitted from the surface of the gamma irradiated material and then synthesizing this distribution by using a linear accelerator beam. From electron beam synthesis of nuclear reactor irradiation experiments, the extent and method by which energetic primary electrons contribute to increased current flow in irradiated diodes could be determined.

The transfer of energy between photons and matter is important in the calculation of energetic electron emission from the surface of an irradiated target. In this energy transfer process, photon energy is converted to kinetic energy of electrons and to rest energy of electron-positron pairs, and then the kinetic energy of the primary electrons is dissipated along their tracks because of interactions with atomic electrons and nuclei. Electrons produced near the surface, however, may not deposit all of this energy and thus be able to escape depending on the spatial location and initial energy of the electron. This report is limited to calculating the current density and energy spectra of these escaping primary electrons.

Gamma ray interactions with matter have been extensively studied, and specifications of the various interaction cross sections have been reported. Descriptions of these processes and data on energy transfer coefficients are found in works by Fano, Spencer, and Berger (ref. 3); Grodstein (ref. 4); Berger (ref. 5); and Evans (ref. 6).

Electron transport through matter and the basic electron interactions which occur during flight are described by Rossi (ref. 7), Bethe and Ashkin (ref. 8), Fano (ref. 9), and Birkhoff (ref. 10). Different calculational techniques and theoretical models have been applied in order to obtain better agreement between calculated results and experimental data. Monte Carlo methods by Berger and Seltzer (ref. 11), the phase-space

time evolution method by Cordaro and Zucker (ref. 12), and the method of discrete ordinates using the code ANISN by Bartine, Alsmiller, Mynatt, Engle, and Barish (ref. 13) represent major efforts in the study of electron transport utilizing high-speed large computers. The main contribution of the work presented in this report lies in the formulation of a simple computational method of estimating electron penetration by using available experimental data.

The numerical results presented are for a tungsten target 0.33 centimeter thick and 2.5 centimeters in diameter irradiated by the fission gamma flux in the core of the NASA Lewis Research Center Plum Brook nuclear test reactor. The spatial distribution of gamma radiation is prescribed according to specifications of geometry and fuel loading of the core. The fission gamma energy spectrum is divided into 13 discrete energy groups, each one characterized by a monoenergetic gamma flux having the mean energy of the group. The generation of primary electrons is deduced from appropriate energy transfer coefficients as a function of gamma energy. The spectrum of primary electron energies resulting from gamma interactions is approximated by an average energy within each specified gamma group. Empirical electron energy-range relations are used in conjunction with the probability of escape and the average path length of escaping electrons to compute the emission of energetic electrons. The derivation of the latter two quantities follow along the lines first suggested by Butler. This approach differs from an earlier calculation by Shiomi and Higashimura (ref. 14), who adapted the penetration theory of Spencer (ref. 15) and the segment theory of Higashimura (ref. 16) in describing electron emission from a plane semi-infinite target results from the passage of a normal incidence gamma flux. The energy spectra and flux of emerging electrons from a uniform plane slab target of finite thickness are calculated by assuming an isotropic, monoenergetic beam of photons for each group. The total emission current density and power per unit area are then computed by summing over the 13 discrete energy groups.

SYMBOLS

B_e binding energy, eV

c speed of light, m/sec

e charge of electron, 1.6×10^{-19} C

$\mathscr{S}_e$ secondary electron energy flux within target, W/cm^2

$\mathscr{S}_\gamma$ gamma energy flux, W/cm^2

J_{esc} current density of escaping secondary electrons, $\mu A/cm^2$

K linear pair production attenuation coefficient, cm^{-1}

m_o electron rest mass, kg

P_{esc} probability of escape for secondary electron

R electron range, g/cm^2

r electron path length defined in fig. 1

T target thickness, g/cm^2

W energy flux of escaping secondary electrons, W/cm^2

x dimension defined in fig. 1

ϵ_e initial energy of electron, eV

ϵ_{esc} energy of electron upon escape from target, eV

ϵ_L energy lost by electron within target, eV

ϵ_γ gamma energy, eV

θ dimension defined in fig. 1

θ_c critical angle for escape

μ_e linear coefficient of gamma energy absorption, cm^{-1}

μ_t total linear gamma energy attenuation coefficient, cm^{-1}

ρ density of target, g/cm^2

σ_a Compton absorption coefficient, cm^{-1}

σ_s Compton scattering coefficient, cm^{-1}

τ photoelectric linear absorption coefficient, cm^{-1}

φ azimuthal angle

PROBABILITY OF ESCAPE

The probability that an electron, generated by photon interaction within a target, will escape to the surface is derived in this section. The target is assumed to be an infinite slab which is immersed in an isotropic monoenergetic gamma flux field. The electrons produced by photoelectric, Compton, or pair production interactions will likewise have an isotropic distribution; however, the electron energy distribution associated with a given gamma energy will be simplified by assuming each electron has an energy equal to the average. The methods and implications of this averaging process are discussed in the section CALCULATION OF EMITTED ELECTRON CURRENT.

Since the cross section is large, electron-electron scattering is the major mechanism of energy degradation of the primary electron as it traverses the medium. It is because of the almost continuous loss of energy in multiple electron-electron interactions that primary electrons have an almost precise range R. For a target whose thickness is greater than the range of the scattered electrons, the escape probability is different from that for a target of smaller thickness. The derivation is best begun by reference to figure 1.

The line r in figure 1 does not represent as escape path for an electron generated by x'. In traversing the medium to the surface, electrons will lose energy in numerous collisions, and as a result the escape path will deviate considerably from a straight line.

The differential probability of escape dP_{esc} for an electron scattered between $x = x' + dx$ and $x = x'$ in an infinite slab is the fraction of the solid angle of the sphere of radius R contained within the cone $\theta \leq \theta_c$:

$$dP_{esc} = \frac{1}{4\pi} \int_0^{\theta_c} \int_0^{2\pi} \sin\theta \, d\varphi \, d\theta \tag{1}$$

The total probability of escape from one side of the target where the thickness is greater than the range is obtained by averaging dP_{esc} throughout the target:

$$P_{\substack{esc \\ T \geq R}} = \frac{\displaystyle\int_{T-R}^{T} \int_0^{\theta_c} \int_0^{2\pi} \frac{\sin\theta}{4\pi} \, d\varphi \, d\theta \, dx}{\displaystyle\int_0^{T} dx} = \frac{R}{4T} \tag{2}$$

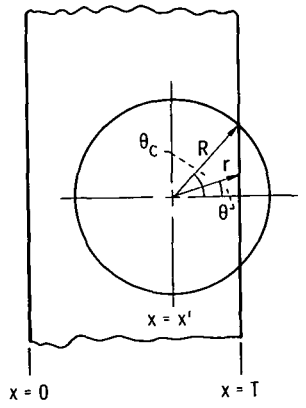

Figure 1. - Diagram for computing probability of escape for electron scattered at x' in target of thickness T.

When the thickness of the target is less than the range, the probability of escape from one of the surfaces may be written

$$P_{\substack{esc \\ T<R}} = \int_0^T \int_0^{\theta_c} \int_0^{2\pi} \frac{\sin\theta}{4\pi T} \, d\varphi \, d\theta \, dx = \frac{1}{2}\left(1 - \frac{T}{2R}\right) \tag{3}$$

AVERAGE PATH LENGTH FOR ESCAPING ELECTRONS

When the thickness of the target is greater than the electron range R, as shown in figure 1, the path length R of electrons escaping from one side of the slab from x, where T - x is less than the range, will be a function of the scattering angle θ:

$$r = \frac{T - x}{\cos\theta} \tag{4}$$

The mean path length of escaping electrons is computed by averaging r over the pertinent ranges of x, φ, and θ:

$$\bar{r} = \frac{\displaystyle\int_{T-R}^{T} \int_0^{\theta_c} \int_0^{2\pi} \frac{T - x}{\cos\theta} R^2 \sin\theta \, d\varphi \, d\theta \, dx}{\displaystyle\int_{T-R}^{R} \int_0^{\theta_c} \int_0^{2\pi} R^2 \sin\theta \, d\varphi \, d\theta \, dx} \tag{5}$$

where

$$\theta_c = \cos^{-1}\frac{T - x}{R}$$

After the appropriate substitutions, the integral (5) can be solved for $T > R$ to obtain the simple result

$$\bar{r} = \frac{R}{2} \tag{6}$$

For thin targets ($R > T$) the integral (5) is equally valid with the modification that the limits of integration on x are from 0 to T.

The average path length of electrons escaping from one side of the target is

$$\bar{r} = \frac{T}{2} \frac{\ln \frac{R}{T} + \frac{1}{2}}{1 - \frac{T}{2R}} \tag{7}$$

CALCULATION OF EMITTED ELECTRON CURRENT

The quantities which must be known for the computation of high-energy electron emission from a target in a gamma flux field are the gamma energy ϵ_γ, the gamma energy flux $\mathcal{J}_\gamma$, the target density ρ, the total linear gamma energy attenuation coefficient μ_t, and the linear coefficient of absorption of gamma energy electrons μ_e. The development will be restricted to targets thicker than the average electron range.

Even a monoenergetic gamma flux field will produce electrons with a wide spectrum of energies. In this calculation, the distribution of electron energies is approximated by an electron flux of constant energy equal to the average. This first step in the calculation is to find the average energy $\bar{\epsilon}_e$ of the electrons resulting from the attenuation of the gamma flux in the target. When μ_e and μ_t are known, the equation for $\bar{\epsilon}_e$ may be written

$$\bar{\epsilon}_e = \epsilon_\gamma \frac{\mu_e}{\mu_t} \tag{8}$$

When tabulated values of μ_e and μ_t are not available or when a theoretical analysis of the energy absorption process is desired, equation (8) may be expressed (ref. 6)

$$\bar{\epsilon}_e = \epsilon_\gamma \frac{\sigma_a + \tau\left(1 - \frac{B_e}{\epsilon_\gamma}\right) + K\left(1 - \frac{2m_oC^2}{e\epsilon_\gamma}\right)}{\sigma_a + \sigma_s + \tau + K} \tag{9}$$

where σ_a is the Compton absorption coefficient, τ is the photoelectric linear absorption coefficient, B_e the binding energy of the target atoms, K the linear pair production

attenuation coefficient, m_0 the rest mass of the electron, e the electronic charge, c the speed of light, and σ_s the Compton scattering coefficient.

The extrapolated range R of the electrons produced as a result of photon interactions in the target is found in the literature for the appropriate material and energy (refs. 17 to 19). The range-energy relation for tungsten taken from reference 17 is plotted in figure 2.

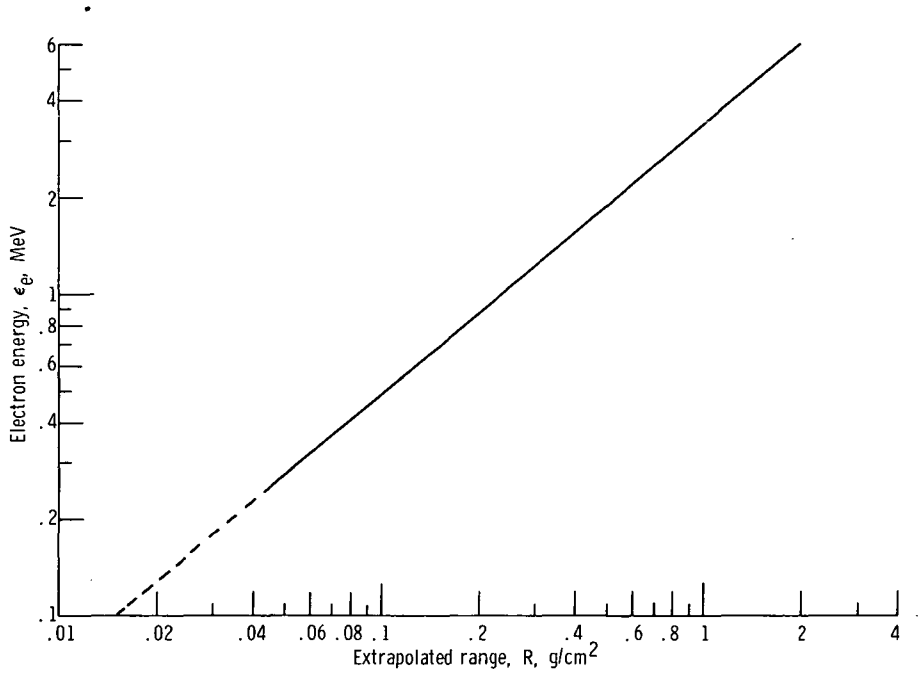

Figure 2. - Energy-range relation for tungsten.

The gamma energy flux drops off exponentially as it penetrates the target material (ref. 6). The primary electrons produced do not have as great a penetration distance as the gamma rays, so that

$$\frac{R}{\rho} << \frac{1}{\mu_e} \tag{10}$$

Therefore, the power per unit area $\mathscr{P}_e$ absorbed by the electrons within a distance R/ρ from the surface may be expressed approximately as

$$\mathscr{P}_e = \mathscr{P}_\gamma \Big|_s \left(\frac{R\mu_e}{\rho}\right) \tag{11}$$

For the thick targets treated in this report the average path length $\bar{r}$ of escaping electrons is shown in equation (6) to be R/2. The average energy loss $\bar{e}_L$ for electrons can then be found from figure 2. The average energy $\bar{\epsilon}_{esc}$ of escaping electrons is then computed from

$$\bar{\epsilon}_{esc} = \bar{\epsilon}_e - \bar{\epsilon}_L \tag{12}$$

The energy flux W of escaping energetic electrons can now be written

$$W = \frac{\mathcal{J}_e \bar{\epsilon}_{esc} P_{esc}}{\bar{\epsilon}_e} \tag{13}$$

Ideally, the escape of electrons from a depth greater than one range is not possible; hence, only that portion of the target which is one range thick need be considered. From equation (2) the probability of escape is simply 1/4, so that equation (13) may be written

$$W = \frac{\mathcal{J}_e \bar{\epsilon}_{esc}}{4\bar{\epsilon}_e} \tag{14}$$

Finally, the escape current density $\bar{J}_{esc}$ is simply expressed as

$$\bar{J}_{esc} = \frac{\mathcal{J}_e}{4\bar{\epsilon}_e} \tag{15}$$

RESULTS FOR TUNGSTEN

The calculation presented in this section refers to a tungsten target 0.33 centimeter thick placed within the gamma flux field approximately 4 centimeters from the core of the NASA Plum Brook Reactor. This system is of interest because of its possible application to a thermionic converter designed to operate within the core of a nuclear reactor.

The gamma flux distribution at the point of interest was obtained by using the computer code QAD P5A (refs. 20 and 21) and the gamma energy spectrum of Groshev (ref. 22). The gamma energy spectrum of a nuclear reactor is nearly continuous and not a monoenergetic beam as called for in the computation; however, by splitting the spectrum into 13 energy groups, the average energy and energy flux of each may be specified. This is done in table I, second and third columns. The linear attenuation and absorption coefficients are obtained from published data (ref. 23) and for convenience

TABLE I. - SCHEDULE OF COMPUTATION FOR TUNGSTEN TARGET 0.33 CENTIMETER THICK

Group	Gamma energy, $\bar{\epsilon}_\gamma$, MeV	Gamma energy flux, $\mathcal{F}_\gamma$, W/cm^2	Ratio of absorption to attenuation coefficient, μ_e/μ_t	Electron energy, $\bar{\epsilon}_e$, MeV	Electron range, R, g/cm^2	Ratio of absorption coefficient to target density, μ_e/ρ, cm^2/g	Secondary electron energy flux within target, $\mathcal{F}_e$, W/cm^2	Energy lost by electron within target, $\bar{\epsilon}_L$, MeV	Electron escape energy, $\bar{\epsilon}_{esc}$, MeV	Energy flux of escaping secondary electrons, $\bar{W}$, W/cm^2	Current density of escaping secondary electrons, $\bar{J}_{esc}$, μA cm^2	Normalized energy flux of escaping electrons, $(\bar{W}/\mathcal{F}_\gamma)\times 100$, percent
1	0.267	1.582	0.82	0.219	0.038	0.305	0.0183	0.123	0.096	0.0020	0.0208	0.126
2	.618	29.149	.59	.365	.0705	.0570	.117	.205	.160	.0128	.0800	.044
3	1.119	34.772	.55	.615	.132	.0310	.142	.345	.270	.0156	.0578	.045
4	1.572	32.701	.58	.912	.212	.0280	.194	.510	.402	.0214	.0532	.065
5	1.995	26.893	.63	1.257	.310	.0270	.225	.740	.517	.0231	.0447	.086
6	2.394	20.597	.665	1.592	.415	.0275	.235	.900	.692	.0255	.0369	.124
7	2.792	17.942	.695	1.940	.520	.0284	.265	1.080	.86	.0294	.0342	.164
8	3.235	16.602	.725	2.345	.660	.0295	.323	1.320	1.025	.0353	.0344	.213
9	3.74	12.053	.76	2.842	.830	.0305	.305	1.600	1.242	.0333	.0268	.276
10	4.228	8.696	.785	3.319	1.000	.0315	.274	1.870	1.449	.0299	.0206	.344
11	4.735	5.554	.807	3.821	1.190	.0325	.215	2.150	1.671	.0235	.0141	.423
12	5.230	3.640	.827	4.325	1.375	.0335	.168	2.450	1.875	.0182	.0097	.500
13	6.334	5.706	.86	5.447	1.850	.0360	.380	3.100	2.347	.0409	.0174	.717

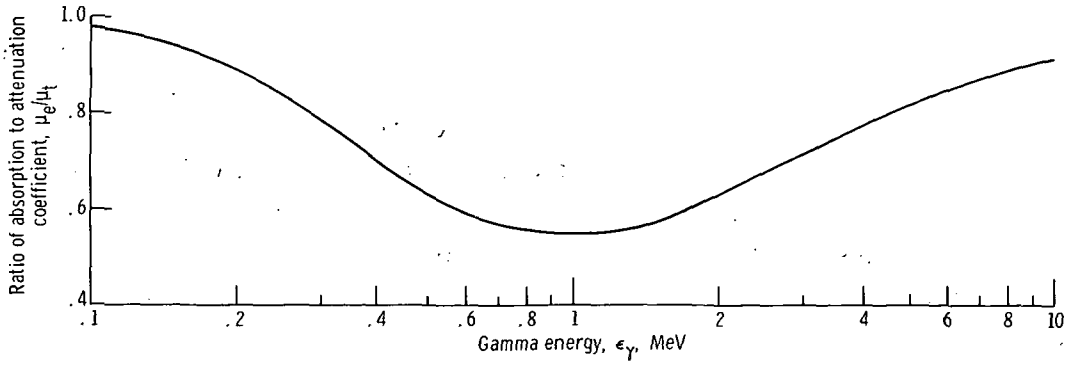

Figure 3. - Ratio of absorption to attenuation coefficient for tungsten.

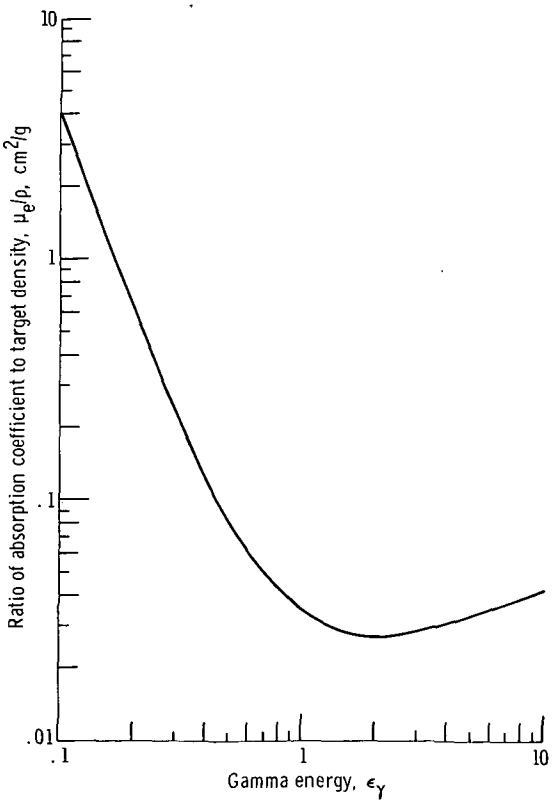

Figure 4. - Absorption coefficient for tungsten.

plotted in figures 3 and 4. The calculation then proceeds as described in the preceding section.

The results of the calculation, the power per unit area and current of escaping electrons, are shown in figures 5 and 6. The totals for all energy ranges are 0.3109 watt per square centimeter and 0.4506 microampere per square centimeter. By comparison, in a cesium-filled thermionic converter operating in the power producing mode, the loss in the plasma is of the order of 5 watt per square centimeter.

This value for the current density of electrons in the million volt energy range has been utilized in experiments in which the effect of gamma radiation is simulated by the electron beam of a linear accelerator. The results of some of these experiments were reported by Bacigalupi (ref. 24) and Forman (ref. 2). In tests of a xenon-filled thermionic diode, excellent agreement was obtained for current, voltage curves taken in a nuclear reactor and in a linear accelerator which was delivering a current density predicted by this method of calculation.

In addition to the primary electrons having energies of the order of 1 MeV, secondary electrons of energy less than 100 volts will also be emitted. These secondary elec-

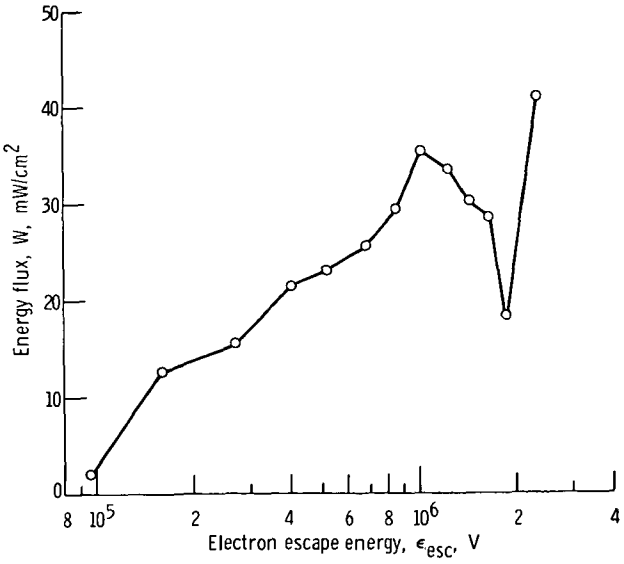

Figure 5. - Energy flux of escaping electrons.

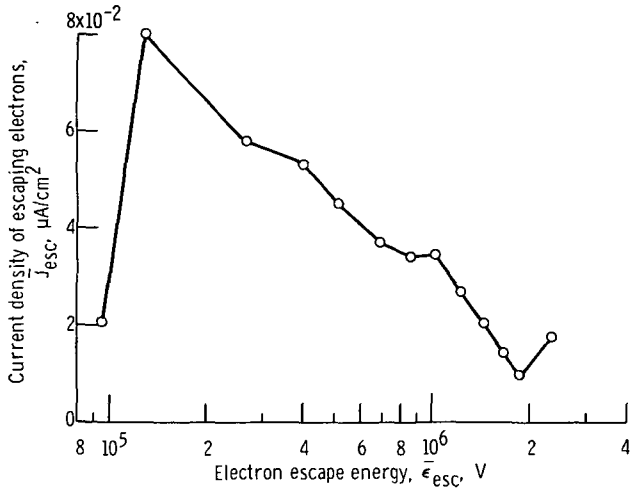

Figure 6. - Current density of escaping electrons.

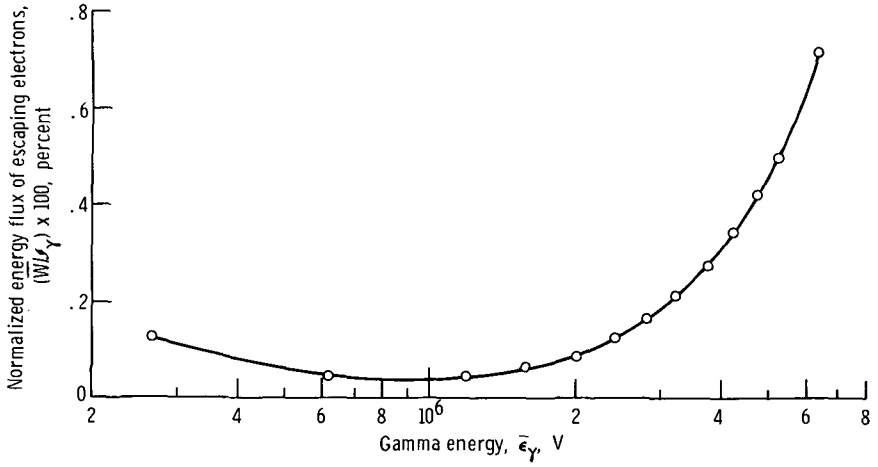

Figure 7. - Normalized energy flux of escaping electrons.

trons have been found to be more numerous than the primary electrons by some investigators (refs. 25 and 26). The effect of the low-energy secondary electrons presumably could in some instances be as important as that of the primary electrons in altering thermionic converter performance.

Of more general interest may be the plot of $W/\mathcal{J}_\gamma$ shown in figure 7. Within the accuracy of the computation, figure 7 should apply to any tungsten target irradiated by a gamma flux field of any specified energy spectrum as long as the thickness of the target is greater than or equal to the range.

The rise in $W/\mathcal{J}_\gamma$ for incident gamma rays above 0.7 MeV can be readily explained. If equations (11) and (12) are substituted into equation (14), an expression is obtained for $W/\mathcal{J}_\gamma$:

$$\frac{W}{\mathcal{J}_\gamma\Big|_s} = \frac{R\mu_e}{4\rho}\left(1 - \frac{\bar{\epsilon}_L}{\bar{\epsilon}_e}\right) \tag{16}$$

As the gamma energy is increased, the range increases and the ratio of electron energy lost to original electron energy decreases, both factors tending to increase $W/\mathcal{J}_\gamma$. The absorption coefficient, figure 4, drops rapidly up to about 2 MeV and then increases slowly for higher values of ϵ_γ and thus accounts for the shape of figure 7.

It should be emphasized once more that figure 7 applies only to the case where range does not exceed target thickness. Therefore, for any target of finite thickness the ratio of W to $\mathcal{J}_\gamma$ will not increase indefinitely for incident gammas of higher energy.

SUMMARY OF RESULTS

This report presents a method for estimating the emission of high-energy electrons from a metal target irradiated in a gamma flux field. The calculation was based on photon energy-transfer coefficients, the electron energy range relations, the probability of electron escape, and the average path length of emitted electrons. The latter two quantities were derived in this report.

The magnitude of electron current density and energy flux resulting from the placement of a tungsten target in the gamma radiation field of a nuclear reactor was computed. In this numerical example, the continuous gamma energy spectrum was broken into 13 monoenergetic groups, and the photon, electron interactions were treated for each group separately. For a 0.33-centimeter-thick tungsten target located 4 centimeters from the core of the NASA Plum Brook Reactor, a total primary current density of

0.4506 microampere per square centimeter and an energy flux of 0.3109 watt per square centimeter were estimated.

This calculation has been used successfully to predict a starting point for the simulation with the beam of a linear accelerator an effect observed in a nuclear reactor. The agreement between reactor and linear accelerator data reported so far may be fortuitous, considering the many approximations on which this calculation was based. The results obtained should be taken only as an estimate of the million-volt-electron emission caused by the gamma radiation.

Lewis Research Center,
National Aeronautics and Space Administration,
Cleveland, Ohio, December 26, 1972,
503-25.

REFERENCES

1. Butler, D.: Gamma-Ray Ionization in the Plasma Diode. Adv. Energy Conversion, vol. 4, no. 1, Jan.-Mar. 1964, pp. 39-50.
2. Forman, Ralph: Electrical Properties of Xenon-Filled Thermionic Diodes in the Radiation Field of a Nuclear Reactor. J. Appl. Phys., vol. 39, no. 9, Aug. 1968, pp. 4351-4355.
3. Fano, U.; Spencer, L. V.; and Berger, M. J.: Penetration and Diffusion of X-Rays. Neutrons and Related Gamma Ray Problems. Vol. XXXVIII/2 of Handbuch der Physik. S. Flügge, ed., Springer-Verlag, 1959, pp. 60-868.
4. Grodstein, Gladys Wh.: X-Ray Attenuation Coefficients from 10 KeV to 100 MeV. Circ. 583, National Bureau of Standards, Apr. 30, 1957.
5. Berger, Rosemary T.: The X- or Gamma-ray Energy Absorption or Transfer Coefficient: Tabulations and Discussion. Radiation Res., vol. 15, no. 1, July 1961, pp. 1-29.
6. Evans, Robley D.: The Atomic Nucleus. McGraw-Hill Book Co., Inc., 1955.
7. Rossi, Bruno B.: High-Energy Particles. Prentice-Hall, Inc., 1952.
8. Bethe, H. A.; and Ashkin, J.: Passage of Radiation Through Matter. Experimental Nuclear Physics. Vol. 1. E. Segre ed., Johy Wiley & Sons, Inc., 1953.
9. Fano, U.: Degradation and Range Straggling of High-Energy Radiations. Phys. Rev., vol. 92, no. 2, Oct. 15, 1953, pp. 328-349.

10. Birkhoff, R. D.: Handbuch der Physik. Vol. 34. S. Flügge ed., Springer-Verlag, 1958.

11. Berger, M. J.; and Seltzer, S. M.: ETRAN, Monte Carlo Code System for Electron and Photon Transport Through Extended Media. Rep. NBS-9836 and NBS-9837, National Bureau of Standards, 1968.

12. Cordaro, Matthew C.; and Zucker, Martin S.: A Method for Solving Time-Dependent Electron Transport Problems. Nucl. Sci. Eng., vol. 45, no. 2, Aug. 1971, pp. 107-116.

13. Bartine, D. E.; Alsmiller, R. G., Jr.; Mynatt, F. R.; Engle, W. W., Jr.; and Barish, J.: Low-Energy Electron Transport by the Method of Discrete Ordinates. Nucl. Sci. Eng., vol. 48, no. 2, June 1972, pp. 159-178.

14. Shiomi, Naoko; and Higashimura, Takenobu: Calculation of the Secondary Electron Spectrum at the Boundary Layer. Japanese J. Appl. Phys., vol. 2, no. 7, July 1963, pp. 406-409.

15. Spencer, L. V.: Theory of Electron Penetration. Phys. Rev., vol. 98, no. 6, June 15, 1955, pp. 1597-1615.

16. Higashimura, T.: Electron Penetration Through Aluminum. Radiation Res., vol. 2, 1961, pp. 1-19.

17. Wittig, Siegmar: A Universal Monte Carlo Method for the Solution of Electron Transport Problems. Rep. ORNL-TR-2126, Oak Ridge National Lab., 1968.

18. Miller, William E.: Transmission and Backscatter Coefficients of 1.0- to 3.0-MeV Electrons Incident on Some Metals and Alloys. NASA TN D-5724, 1970.

19. Tabata, Tatsuo; Ito, Rinsuke; Okabe, Shigeru; and Fujita, Yoshiaki: Extrapolated and Projected Ranges of 4- to 24-MeV Electrons in Elemental Materials. J. Appl. Phys., vol. 42, no. 9, Aug. 1971, pp. 3361-3366.

20. Malenfant, Richard E.: QAD, A Series of Point-Kernel General-Purpose Shielding Codes. Rep. LA-3573, Los Alamos Scientific Lab., Apr. 5, 1967.

21. Lahti, Gerald P.: QADHD Point-Kernel Radiation Shielding Computer Code to Evaluate Propellant Heating and Dose to Crew During Engine Operation. NASA TM X-1397, 1967.

22. Groshev, L. V.; and Demidov, A. M.: Gamma-Ray Spectrum of the IRT Reactor. Soviet J. Atomic Energy, vol. 7, no. 3, Mar. 1961, pp. 748-749.

23. Anon.: Reactor Physics Constants. Rep. ANL-5800, Argonne National Lab., 1958.

24. Bacigalupi, Robert J.: Simulation of In-Pile Effects on Thermionic Diodes. NASA TM X-52713, 1969.

25. Cohen, Allan J.; and Koral, Kenneth F.: Backscattering and Secondary-Electron Emission from Metal Targets of Various Thicknesses. NASA TN D-2782, 1965.

26. Frederickson, A. R.; and Burke, E. A.: Ionization, Secondary Emission, and Comptron Currents at Gamma Irradiated Interfaces. IEEE Trans. on Nucl. Sci., vol. NS-18, no. 6, Dec. 1971, pp. 162-129.

NASA-Langley, 1973 —— 24 E-7265

NATIONAL AERONAUTICS AND SPACE ADMINISTRATION
WASHINGTON, D.C. 20546

OFFICIAL BUSINESS
PENALTY FOR PRIVATE USE $300

SPECIAL FOURTH-CLASS RATE
BOOK

POSTAGE AND FEES PAID
NATIONAL AERONAUTICS AND
SPACE ADMINISTRATION
451

U.S.MAIL

POSTMASTER : If Undeliverable (Section 158 Postal Manual) Do Not Return

"The aeronautical and space activities of the United States shall be conducted so as to contribute . . . to the expansion of human knowledge of phenomena in the atmosphere and space. The Administration shall provide for the widest practicable and appropriate dissemination of information concerning its activities and the results thereof."

—NATIONAL AERONAUTICS AND SPACE ACT OF 1958

NASA SCIENTIFIC AND TECHNICAL PUBLICATIONS

TECHNICAL REPORTS: Scientific and technical information considered important, complete, and a lasting contribution to existing knowledge.

TECHNICAL NOTES: Information less broad in scope but nevertheless of importance as a contribution to existing knowledge.

TECHNICAL MEMORANDUMS: Information receiving limited distribution because of preliminary data, security classification, or other reasons. Also includes conference proceedings with either limited or unlimited distribution.

CONTRACTOR REPORTS: Scientific and technical information generated under a NASA contract or grant and considered an important contribution to existing knowledge.

TECHNICAL TRANSLATIONS: Information published in a foreign language considered to merit NASA distribution in English.

SPECIAL PUBLICATIONS: Information derived from or of value to NASA activities. Publications include final reports of major projects, monographs, data compilations, handbooks, sourcebooks, and special bibliographies.

TECHNOLOGY UTILIZATION PUBLICATIONS: Information on technology used by NASA that may be of particular interest in commercial and other non-aerospace applications. Publications include Tech Briefs, Technology Utilization Reports and Technology Surveys.

Details on the availability of these publications may be obtained from:

SCIENTIFIC AND TECHNICAL INFORMATION OFFICE

NATIONAL AERONAUTICS AND SPACE ADMINISTRATION

Washington, D.C. 20546